IMPROVED LIMIT ON THE ELECTRON ANTI NEUTRINO REST MASS FROM TRITIUM β-DECAY

Ch.Weinheimer, M.Przyrembel, H.Backe, H.Barth, J.Bonn B.Degen, Th.Edling, H.Fischer, L.Fleischmann, J.U.Grooß, R.Haid, A.Hermanni, G.Kube, P.Leiderer[1], Th.Loeken, A.Molz, R.B.Moore[2], A.Osipowicz, E.W.Otten, A.Picard, M.Schrader, M.Steininger
Institut für Physik, Universität Mainz, Germany

Presented by J.Bonn

ABSTRACT

The endpoint region of the β-spectrum of tritium was remeasured by an electrostatic spectrometer with magnetic guiding field. It enabled the search for a rest mass of the electron anti neutrino with improved precision. The result is $m_\nu^2 = (-39 \pm 34_{stat} \pm 15_{syst})(eV/c^2)^2$, from which an upper limit of $m_\nu < 7.2eV/c^2$ may be derived. The experiment yields the atomic mass difference $m(T) - m(^3He) = (18591 \pm 3)eV/c^2$.

Present addresses:

[1] Fakultät für Physik, Universität Konstanz, Germany
[2] Mc Gill University, Montreal, Canada

In former Moriond conferences we presented progress reports in design and test of a solenoid retarding spectrometer [1, 2] dedicated to study the endpoint of the T_2 β-decay spectrum. First preliminary results were presented in 1991 and 1992. This report gives the first full data analysis yielding a new upper limit on the electron anti neutrino rest mass [3]. The principle of the spectrometer is briefly explained in Fig.1. Due to the adiabatic transforma-

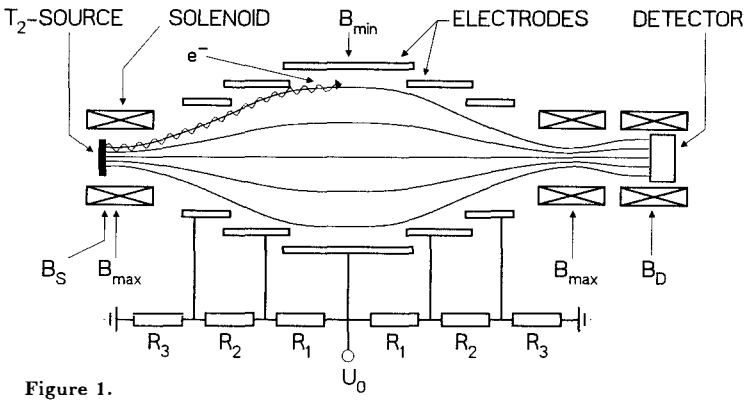

Figure 1.

Principle of the solenoid retarding spectrometer. Electrons emitted from the T_2 source are magnetically guided to the detector. The gradient force $F_\nabla = (\vec{\mu} \times \vec{\nabla}) \times \vec{B}$, acting on the orbital magnetic moment $\vec{\mu}$ of the electrons transforms energy $E_\perp$ in the cyclotron motion around the magnetic field lines into longitudinal motion parallel to the magnetic field. $E_\parallel$ is electrostatically analyzed in the symmetry plane of the spectrometer.

tion of energy in the cyclotron motion $E_\perp$ around the magnetic field lines into $E_\parallel$ parallel to the magnetic field the full foreward solid angle can be accepted. The filter width under these conditions is given by $\Delta E = B_1/B_0 \cdot E$, where B_0 is the maximum and B_1 is the minimum magnetic field.

The experiment described here was performed under the following conditions. The source is placed at a field $B_S = 0.96\ B_0$, slightly in front of the field maximum of the source solenoid which is set to $B_0 = 2.4$ T, limiting the accepted polar angles to $\vartheta < 78°$. The magnetic field reaches its minimum $B_1 = 8 \cdot 10^{-4} T$ in the symmetry plane of the spectrometer, where U_0 maximizes. Retardation of the electrons and reacceleration after the filter is provided by two sets of electrodes arranged symmetrically around the central one. Under these conditions the rise of the transmission from 0 to 1 within the interval $E(1 - B_1/B_0) \leq e \cdot U_d \leq E$ is given by [14]:

$$T(E,U_d) = \frac{1 - \sqrt{1 - \dfrac{E - e \cdot U_d}{E} \cdot \dfrac{B_S}{B_1}}}{\left(1 - \sqrt{1 - \dfrac{B_S}{B_0}}\right)} \qquad (1)$$

where $U_d = U_S - U_0$ is the difference between the potentials of the source and the central electrode. $T(E,U_d)$ was checked with high accuracy by conversion electrons from ^{83m}Kr [14]. As important as the sharpness of the filter is the absence of any tails of $T(E,U_d)$ extending

beyond E. During reacceleration, the electrons are also refocussed by the field of a second solenoid, also set to 2.4 T, and finally reach a silicon detector placed in the central field B_D = 0.8 T of a third solenoid. The active area of the detector has a diameter of 25 mm and is segmented into five rings of equal area. The counts were pulse height analyzed and stored event by event. Cooled down to $-80°C$, the detector has a resolution of 2.0 keV FWHM for 20 keV electrons. The resolution was somewhat degraded with respect to the values reported in ref. [15] due to 15 $\mu g/cm^2$ aluminium evaporated onto the $30\mu g/cm^2$ Kapton foil separating the high vacuum at the detector from the UHV in the spectrometer.

Regarding the source, we decided on molecular T_2 frozen onto an aluminium substrate cooled down to 2.8 K. Compared to any other T-compound, this choice offers the highest specific activity. Because of the lowest possible Z, the spectrum of energy losses by inelastic scattering within the source, as well as by prompt shake up/off processes, is, in comparison, also soft and simple. According to extensive molecular orbit calculations [16], the final state spectrum of the latter is slightly more complicated than that of gaseous T_2 [17]. The present source was constructed following the experience of a feasibility study [18]. The substrate is mounted on the front of a 1.2 m long, horizontal LHe cryostat. The solid angle of T_2- evaporation into the spectrometer is limited to $\Delta\Omega/4\pi = 2.5 \cdot 10^{-3}$ by a LHe-cooled, 10 cm long and 2 cm wide Cu tube in front of the source which itself covers a circular area of 1 cm^2. The tube also reduces condensation of residual gas onto the source. The source is connected to the spectrometer by a bellows allowing it to be moved from the loading to the measuring position through a valve. T_2 is evaporated onto the substrate by covering the respective area with a teflon cup into which T_2 is led through a capillary. Glass windows allow the evaporation process to be controlled by ellipsometry. Films of 40 monolayers, corresponding to a total source strength of 10^8 Bq were prepared. Through on line mass spectrometry we detected tritium contaminations of about 30 % of hydrogen which had probably taken place in the stainless steel container.The source region meets the UHV conditions of the spectrometer [1]. During measurements the source "decayed" almost exponentially with a half-life time of a week. Data were taken for about ten days per source.

Without a source the background spectrum peaked at about 23 keV, well above the tritium spectrum [1]. Therefore, most of it could be suppressed by limiting the window of accepted events between 12 and 19.5 keV. The residual background rate then dropped to 5 mHz for the central segment and to 23 mHz for the outermost one. With the tritium source the background rate rose by a factor of up to 2 for a fresh source. This additional background peaked at the energy $-e \cdot U_0$. A rough estimation showed that it could be attributed to T_2 molecules which evaporate from the source and decay in vacuo within the magnetic flux tube projected onto the detector. After removing the source the background rate returned immediately to the original value showing no obvious sign of contamination of the spectrometer.

Tritium spectra were recorded in the energy interval $18095eV \leq e \cdot U_d \leq 18800eV$ by scanning up and down a negative potential U_S on the source[3] at constant analyzing potential U_0 = -18779 V. The most critical region around the endpoint was scanned in steps of 4 V with an integration time of $2 \cdot 30s$ per point and scan. Elsewhere larger steps and shorter integration times were chosen. The data were screened for false events. By checking the distribution of time differences between events we detected sudden increases in the count rate, possibly triggered by microsparks in the spectrometer. About 14 % of the whole set of about 500 scans have been rejected due to this failure. The scatter of the remaining data obeys a statistical distribution. Fig.2 shows the recorded β-spectrum. The data comprise counts of the two innermost segments

[3] Negative source potential is essential for retaining ions from T_2 decay which are otherwise accelerated into the spectrometer causing a few Hz background rate by ionization of residual gas.

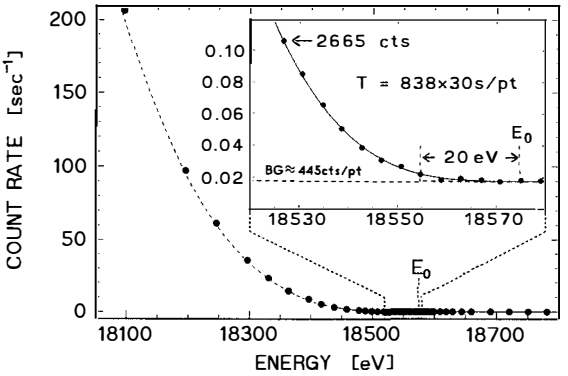

Figure 2.

β-spectrum of tritium recorded during a four week run in 1991. The statistical error bars are too small to be plotted. For energies $E_e \geq 18460eV$ the integral measuring time is 25140s per point. The background level is 450 cts per point ≙18mHz. The full line is the best fit to the data in the interval from 18438 eV to 18800 eV, the broken one is the extrapolation of the fit to lower energies.

of the detector. The other ones are covered only partly by the image of the source and suffer from higher background. An expanded view of the endpoint region is given in the insert. Already 20 eV below the endpoint, the spectrum emerges clearly from the background noise.

Another instructive view to the data is obtained from a linearized plot of the spectrum given in fig.3. Since our spectrometer is integrating the β-spectrum, the linearization is achieved to a first approximation by the cube root of the count rate after substracting the background. The data deviate from the linear slope as soon as transitions to exited states of $(^3HeT)^+$ become significant. The straight line representing transitions to the ground state of $(^3HeT)^+$ intersects the baseline about 4 eV below the endpoint. This is mainly due to the average residual energy in the motion of the electrons around their guiding field lines which is not analyzed by the SRS. The fit, described below, on the other hand slightly overshoots the endpoint, as the best fit value for m_ν^2 is negative. Furthermore, we have plotted into fig.3 fits to the data with m_ν fixed to 0, 10 and 20 eV/c^2 respectively. A value of the order of 20 eV/c^2 is excluded apparently. As to our knowledge, it is the first time that such fine details have ever been resolved in a β-spectrum. In the final evaluation the data were fitted to the sum of a background function

$$b(U_d) = b_0 + b_1 \cdot (E_0 - e \cdot U_d) \tag{2}$$

and a convolution

$$I(U_d) = \int\int T(E', U_d) \cdot D(E', U_d) \cdot L(E, E') \cdot S(E)\, dE \cdot dE' \tag{3}$$

of the transmission function of the spectrometer $T(E', U_d)$ (eq.1), the detector efficiency function $D(E', U_d) = 1 + \alpha_D(E' - eU_d)$ with $\alpha_D = 0.10 \pm 0.01\ keV^{-1}$, the energy loss function L(E,E') and the spectral function of the β-decay S(E).

The background is entirely determined by the data measured beyond E_0 yielding $b_0 = 17.7\ (2)\ mHz$, $b_1 = 5\ (3)\ \mu Hz/V$.

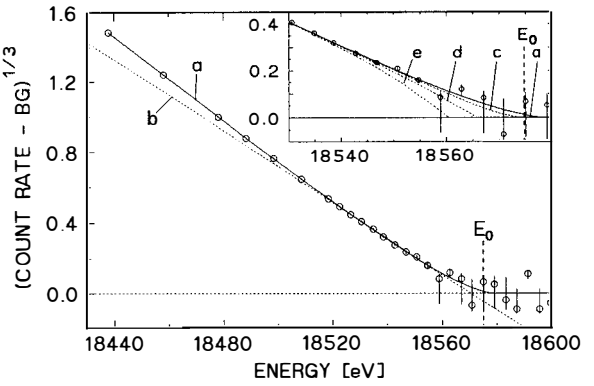

Figure 3.

Linearized β-spectrum close to the endpoint. a: best fit with $m_\nu^2 c^4 = -39 \pm 34 (eV)^2$ and experimental β-endpoint $E_0 = 18574.8 \pm 0.6 eV$, b: linear fit of last 50 eV, c-e: fits with $m_\nu c^2$ fixed to 0, 10, 20 eV in the interval 18438 eV to 18600 eV.

The energy loss function of the sources L(E,E') has been calculated from an inelastic cross section which is approximated by

$$\frac{d\sigma(E,E')}{dE'} = \frac{a_{exc} \cdot \Gamma_{exc}^2}{\Gamma_{exc}^2 + (\Delta E - E_{exc})^2} \cdot \Theta(\Delta E - E_{min}) \cdot \Theta(E_B - \Delta E) + \frac{a_{ion} \cdot \Gamma_{ion}^2}{\Gamma_{ion}^2 + (\Delta E - E_{ion})^2} \cdot \Theta(\Delta E - E_B) \quad (4)$$

with $\Delta E = E - E'$, $E_{min} = 8.8\ eV$, $E_B = 15.4\ eV$,
$a_{exc} = 7.5 \cdot 10^{-19}\ cm^2/(eV \cdot molecule)$, $\Gamma_{exc} = 0.8\ eV$, $E_{exc} = 12.6\ eV$,
$a_{ion} = 1.5 \cdot 10^{-19}\ cm^2/(eV \cdot molecule)$, $\Gamma_{ion} = 7.1\ eV$, $E_{ion} = 17.2\ eV$.
The first Lorentzian approximates the excitation of T_2 [19], the second the ionisation [20]. The parameters a_{exc} and a_{ion} are chosen to match the total stopping power and the total inelastic cross section [21, 22]. The zero loss fraction of electrons is 91% $\pm$ 4% in the average calculated from eq. 4. The error is dominated by uncertainties in the tritium film thickness and homogeneity.

The spectrum is described by

$$S(E) = A \cdot F \cdot p \cdot (E + m_e \cdot c^2) \cdot \sum_i W_i \cdot \varepsilon_i \cdot \sqrt{\varepsilon_i^2 - m_\nu^2 \cdot c^4} \cdot (1 + \alpha_{BS}/3 \cdot \varepsilon_i) \quad (5)$$

with A = amplitude, F = Fermi function[23], p = electron momentum, $\varepsilon_i = (E_0 - V_i - E)$, W_i=relative transition probability to the i'th molecular final state of excitation energy V_i. The backscatter contribution is convoluted with the spectrum in linear approximation by the last factor in eq. 5 with $\alpha_{BS} = 0.20 \pm 0.05\ keV^{-1}$, which was derived from preliminary test measurements. To enable fitting around $m_\nu^2 = 0$ we use a continuation of the term $\varepsilon_i \cdot \sqrt{\varepsilon_i^2 - m_\nu^2 \cdot c^4}$ into the region $m_\nu^2 < 0$ replacing it by $(\varepsilon_i + \mu \cdot exp(-\varepsilon_i/\mu - 1) \cdot \sqrt{\varepsilon_i^2 - m_\nu^2 \cdot c^4}$ with $\mu = 0.76 \cdot \sqrt{-m_\nu^2 \cdot c^4}$. This continuation is smooth and provides a parabolic χ^2-distribution

around $m_\nu^2 = 0$. To save computing time we have replaced the sum over the final states which comprises the product of the final state spectrum of the daughter molecule $(^3HeT)^+$ [17] and the simultaneously excited closest neighbours [16] by 10 discrete states with appropriated Gaussian widths. This procedure has been checked to be sufficiently precise.

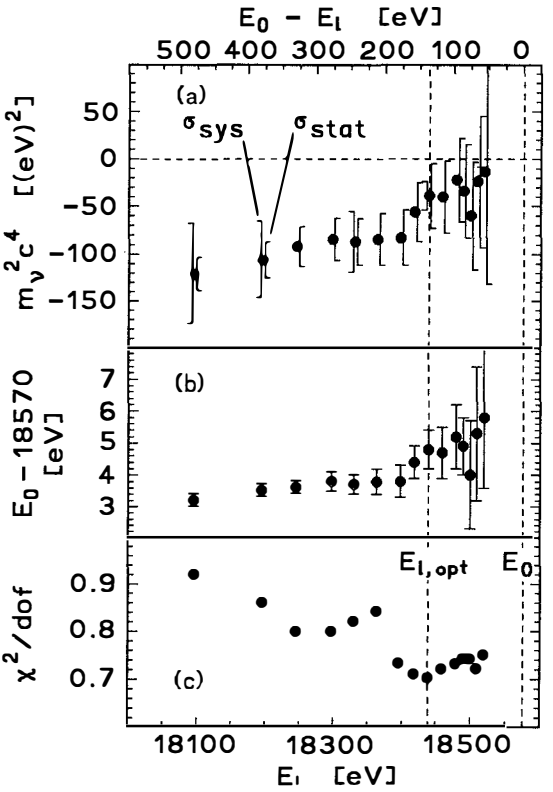

Figure 4.

(a) square of neutrino rest mass m_ν^2, (b) endpoint E_0 and (c) χ^2/dof as function of the lower limit E_l of the fit interval.

The free fit parameters are A, E_0, m_ν^2, b_0 and b_1. Fig.4 shows the best fit results for m_ν^2 , E_0 and χ^2/dof as a function of the lower limit E_l of the fit interval. The significant dependence on this boundary points to residual, systematic errors correlating to m_ν^2 and E_0 further below the endpoint. Although being small they may drag m_ν^2 and E_0 away from the true values because the statistical weight of data points increases rapidly with decreasing energy. As shown by the conservative systematic errors deduced for some of the m_ν-values shown in

fig.4, we believe it unlikely that uncertainties in energy loss, backscatter, spectrometer function etc. could be responsible for this unphysical trend. For $E_l = E_0$ - 137 eV this systematic error is broken down into its components in tab.1. The systematic uncertainties about the final states distribution were checked by using an alternative calculation [29, 30]. The results were essentially unchanged. The trend to negative m_ν^2 arises from an excess count rate far from the endpoint. A simple way to account for this would be to increase the shake off probability. To test this, we changed the shake off probability from 15% as given in ref. [17] over a wide range[4]. At 21% all fit parameters, as well as χ^2/dof, remain stable against variation of the fit interval with m_ν^2 compatible to zero within 1σ statistical error[5].

Table 1. *Influence of variation of critical parameters on m_ν^2 at $E_{l,opt} = E_0 - 137eV$. The coefficients α_D for detector efficiency and α_{BS} for backscatter were changed simultanously since they have the same influence on $I(U_d)$, despite of their different functional dependence. The constant backscatter spectrum was changed by allowing a strong additional linear term keeping the total backscattering probability constant over the interval where the backscatter distribution was investigated. The fraction of energy loss by excitation was changed by 50% while keeping the total inelastic cross section constant. This accounts for different stopping power values given in literature.*

Parameter	Change [%]	$\Delta m_\nu^2 c^4$ $[(eV)^2]$
Inelastic scattering		
total probability	50	14.2
a_{exc} (σ_{tot} =const)	50	3.3
Backscatter & detector eff.		
α_{BS},α_D	25	1.8
different shape	-	3.2
Width of $T(E', U_d)$	10	1.4
Alternative final state		
distribution [29, 30]	-	0.3
Total		15.1

The high resolution and statistics together with the low background of our experiment allow for the first time to reduce the problems associated with including a wider range of the β-spectrum into the data evaluation. We therefore chose $E_{l,opt} = E_0 - 137eV$, where the fraction of ground state transitions is 76 %[6]. The data were fitted for the two sources separately and

[4] Some evidence also seems to exist that shake off probabilities measured in conversion electron spectra [24] exceed calculated ones [25].

[5] An admixture of a second neutrino in the range $m_\nu^2 \leq 100(eV/c)^2$ could remove neither the unphysical value of negative m_ν^2 nor the trends in m_ν^2 and E_0 with increasing data set. In contrast to additional shake off components the inclusion of a second neutrino does not lead to the observed spectral shape due to its essentially different functional dependence.

[6] Extrapolated towards lower energies this fit yields progressively less count rate than measured. When we plot the cube root of this excess count rate (like in Fig.2), a nice, straight Kurie line shows up which intersects with the abscissa 75 eV below the endpoint. Thus it has the signature of a missing spectral component with that endpoint and an amplitude of 4%. We note that the centre of gravity of the shake off electrons is 69 eV.

combined (see tab.2). As a final result we obtain from this interval:

$$m_\nu^2 \cdot c^4 \;=\; (-39 \;\pm\; 34_{stat} \;\pm\; 15_{syst})\;(eV)^2$$

and $E_0 = (18574.8 \pm 0.6) eV$. From E_0 we calculate the mass difference

$$m(T) \;-\; m(^3He) \;=\; (18591 \;\pm 3)\; eV/c^2$$

where the following corrections have been taken into account: recoil energy (1.7 eV), difference in chemical binding energies (16.5 eV), polarization shift (-0.9 eV) [16], difference in work functions between substrate and analyzing electrode (-0.1 eV) [14], potential drop in the analyzing plane (-1.2 eV) [1] . The error is dominated by the uncertainty in the high voltage measurement [14]. Our measurement of the mass difference matches well with recent results [9, 10, 26].

Table 2. *Results for $m_\nu^2/[(eV)^2/c^4]$, $E_0/[eV]$ and χ^2/dof for the two sources S1, S2 and the combined fit Σ.*

	$m_\nu^2 \pm \Delta m_\nu^2$	$E_0 \pm \Delta E$	χ^2/dof
S1	-46 ± 56	18574.2 ± 0.7	0.93
S2	-29 ± 43	18575.3 ± 0.8	0.93
Σ	-39 ± 34	18574.8 ± 0.6	0.70

Following the recipe of the Particle Data Group [27] we calculate from our m_ν^2-result the following upper limit for the electron anti neutrino rest mass with 95 % confidence level:

$$m_\nu \;<\; 7.2\; eV/c^2.$$

In tab.3 we have listed recent measurements of m_ν^2.

Table 3. *Recent results of $m_\nu^2/[(eV)^2/c^4]$ from tritium β-decay. Values of σ_{stat} and σ_{sys} are 1 σ errors. Upper limits on $m_\nu/[eV/c^2]$ according to [27] correspond to 95% c.l.*

Ref.	$m_\nu^2 \pm \sigma_{stat} \pm \sigma_{sys}$	m_ν
LANL [9]	$-147 \pm 68 \pm 41$	< 9.3
Zürich [10]	$-24 \pm 48 \pm 61$	< 11
INS [28]	$-65 \pm 85 \pm 65$	< 13
LLNL [31]	$-60 \pm 36 \pm 30$	< 8
This paper	$-39 \pm 34 \pm 15$	< 7.2

Among the known sources of the systematic error of the present result, uncertainties in the energy loss fraction and the backscatter from the substrate dominate. These values will be checked in detail by measurements with electron conversion lines from ^{83m}Kr covered with D_2 layers of known thickness in the near future. The remaining problem of not fully understanding the measured β-spectrum may be circumvented by restricting the analysis to a region very close to the endpoint which may be even smaller than the one used here. The unique capability of

working very close to the endpoint has not been fully exploited in the past. To this end we will considerably improve the statistical accuracy and make an effort to further reduce background.

The spectrometer was financed by the state of Rheinland-Pfalz and the Bundesminster für Bildung und Wissenschaft providing funds for the new Physics building of the University and its equipment. The Deutsche Forschungsgemeinschaft has contributed to the running and personnel costs of the experiment under the contract number OT33-11. We thank V.M.Lobashev for critical discussions while writing this paper. One of us (R.B.Moore) acknowledges a NATO collaborative grant for support of this work.

References

[1] A.Picard, H.Backe, H.Barth, J.Bonn, B.Degen, Th.Edling, R.Haid, A.Hermanni, P.Leiderer, Th.Loeken, A.Molz, R.B.Moore, A.Osipowicz, E.W.Otten, M.Przyrembel, M.Schrader, M.Steininger, Ch.Weinheimer *Nucl. Instrum. Methods* **B63**(1992)345

[2] H.Backe et al., Proceedings of the 16th Moriond Workshops, 137

[3] Ch.Weinheimer et al. *Phys. Lett.* **B 300**(1993)210

[4] V.A.Lubimov, E.G.Novikov, V.Z.Nozik, E.F.Tretyakov, V.S.Kosik *Phys. Lett.* **94B**(1980)266

[5] S.Boris, A.Golutvin, L.Laptin, V.Lubimov, V.Nagovizin, V.Nozik, E.Novikov, V.Soloshenko, I.Tihomirov, E.Tretyakov, N.Myasoedov *Phys. Rev. Lett.* **58**(1987)2019

[6] E.F.Tretyakov *Bull. USSR Acad.Sci.Phys.*Ser.39,No.3(1975)102

[7] M.Fritschi, E.Holzschuh, W.Kuendig, J.W.Petersen, R.E.Pixley, H.Stuessi *Phys. Lett.* **B173**(1986)485

[8] J.F.Wilkerson, T.J.Bowles, J.C.Browne, M.P.Maley, R.G.H.Robertson, J.S.Cohen, R.L.Martin, D.A.Knapp, J.A.Helffrich *Phys. Rev. Lett.* **58**(1987)2023

[9] R.G.H.Robertson, T.J.Bowles, G.J.Stephenson, D.L.Wark, J.F.Wilkerson, D.A.Knapp *Phys. Rev. Lett.* **67**(1991)957

[10] E.Holzschuh, M.Fritschi, W.Kündig *Phys. Lett.* **B287**(1992)381

[11] V.M.Lobashev, A.I.Fedoseyev, D.V.Serdyuk, A.P.Solodukhin *Nucl. Instrum. Methods* **A240**(1985)305

[12] H.Backe, J.Bonn, Th.Edling, H.Fischer, A.Hermanni, P.Leiderer, Th.Loeken, R.B.Moore, A.Osipowicz, E.W.Otten, A.Picard *Phys. Scr.* **T22**(1988)98

[13] S.Balashov, A.Belesev, A.Bleule et al. *Proc. of the II int. symposium on Weak and Electromagnetic Interactions in Nuclei (W.E.I.N.-89) Montreal*(1989)295,Edition Frontiers, France

[14] A.Picard, H.Backe, J.Bonn, B.Degen, R.Haid, A.Hermanni, P.Leiderer, A.Osipowicz, E.W.Otten, M.Przyrembel, M.Schrader,M.Steininger, Ch.Weinheimer *Z. Phys.* **A342**(1992)71

[15] Ch.Weinheimer, M.Schrader, J.Bonn, Th.Loeken, H.Backe *Nucl. Instrum. Methods* **A311**(1992)273

[16] W.Kolos, B.Jeziorski, J.Rychlewski, K.Szalewicz, H.J.Monkhorst, O.Fackler *Phys. Rev.* **A37**(1988)2297

[17] O.Fackler, B.Jeziorski, W.Kolos, H.J.Monkhorst, K.Szalewicz *Phys. Rev. Lett.* **55**(1985)1388

[18] M.Przyrembel, H.Fischer, A.Hermanni, E.W.Otten, P.Leiderer *Phys. Lett.* **A147**(1990)517

[19] J.Geiger *Z. Phys.* **181**(1964)413

[20] A.E.S.Green, T.Sawada *J.Atm.Terr.Phys.* **34**(1972)1719

[21] L.Pages, E.Bertel, H.Joffre, L.Skalventis *Atomic Data* **4**(1972)1

[22] J.W.Liu *Phys. Rev.* **A7**(1973)103

[23] J.J.Simpson *Phys. Rev.* **D23**(1981)649

[24] D.L.Wark, R.Bartlett, T.J.Bowles, A.G.H.Robertson, D.S.Sivia, W.Trela, J.F.Wilkerson, G.S.Brown, B.Crasemann, S.L.Sorensen, S.J.Schaphorst, D.A.Knapp, J.Henderson, J.Tulkki, T.Åberg *Phys. Rev. Lett.* **67**(1991)2291

[25] Th.A.Carlson, C.W.Nestor *Phys. Rev.* **A8**(1973)2887

[26] R.S.Van Dyck, D.L.Farnham, J.Bare, P.B.Schwinberg *Proc. of the* 6^{th} *Int. Conf. on Nuclei far from Stability and* 9^{th} *Int. Conf. on Atomic Masses and Fundamental Constants Bernkastel-Kues*(1992), ed. by K.L.Kratz et al., in print in the IOP conf. series

[27] Particle Data Group *Phys. Lett.* **204B**(1988)69

[28] H.Kawakami, S.Kato, T.Ohshima, S.Shibata, K.Ukai, N.Morikawa, N.Nogawa, K.Haga, T.Nagafuchi, M.Shigeta, Y.Fukushima, T.Taniguchi *Phys. Lett.* **B256**(1991)105

[29] L.Martin et al. *Phys. Lett.* **110A**(1985)95

[30] D.A.Knapp *doctoral thesis, LANL*(1986)

[31] W.Stoefft *contribution to this workshop*